The Effects of ZnO Additive on Sintering Behavior, Microstructural Evolution and Microwave Dielectric Properties of Li_2TiO_3 Ceramics

T. Ebadzadeh*, S. Ghaffari[1], M. Alizadeh[1], K. Asadian[2] and Y. Ganjkhanlou[3]

*t-ebadzadeh@merc.ac.ir

Received: January 2018 **Revised: April 2018** **Accepted: September 2018**

[1] Department of Ceramics, Materials and Energy Research Center, Karaj, Alborz, Iran.

[2] Department of Semiconductors, Materials and Energy Research Center, Karaj, Alborz, Iran.

[3] Department of Physical Chemistry, Faculty of Chemical Technology, University of Pardubice, Pardubice, Czech Republic.

DOI: 10.22068/ijmse.16.1.1

Abstract: *The densification behavior, structural and microstructural evolution and microwave dielectric properties of Li_2TiO_3 + xZnO (x = 0, 0.5, 1, 1.5, 2, 3, and 5 mol%) ceramics have been investigated using X-ray diffraction, field emission scanning electron microscopy, raman spectroscopy and microwave resonant measurement. The Maximum density of 3.33 g/cm³ was obtained in Li_2TiO_3 + 2ZnO ceramic at low sintering temperature of 1100˚C. Scanning electron microscopy investigations revealed good close packing of grains when x = 2 and preferential grain growth when x ≥ 3. The maximum value of Q × f and εr were 31800 GHz and 22.5 in Li_2TiO_3 + 3ZnO and Li_2TiO_3 + 2ZnO compositions, respectively. The observed properties are attributed to the microstructural evolution and grain growth (first case) or high density of the obtained ceramic (second case).*

Keywords: *Li_2TiO_3, ZnO addition, Microwave dielectric properties, Microstructure, Sintering*

1. INTRODUCTION

The rapid development of wireless telecommunication, such as cellular phones, global positioning systems, personal communication, Tactile Internet (5G wireless systems), Internet of Things (IoT), and satellite broadcasting, has attracted extensive studies on the microwave dielectrics materials [1-5]. Development of wireless communication demands search for low cost microwave dielectrics with high quality factor (Q-factor) [6, 7]. For base station applications several ultralow loss microwave dielectric (high Q-factor) systems such as $Ba(Mg_{1/3}Ta_{2/3})O_3$ (BMT), $Ba(Zn_{1/3}Ta_{2/3})O_3$(BZT) and $Ba((ZnCo)_{1/3}Nb_{2/3})O_3$ (BZCN) have been developed, but lowering the price renders the search for new low cost and high Q microwave dielectric ceramics [7].

Li_2TiO_3 with ordered rock salt superstructure in which cationic (001) planes are alternatively occupied by layers of Li and ($LiTi_2$) layers [8] is a promising microwave dielectric candidate with good quality factor, Q × f > 15000 GHz [8, 9], moderate dielectric constant ~ 22 and τf value of 20.3 ppm/◦C [10-13]. Li_2TiO_3 exists in three modifications: the metastable cubic α-phase which can be synthesized hydrothermally and is stable at low temperatures but transforms irreversibly to monoclinic β-phase between 300 and 600 °C and is stable up to 1150–1215 ˚C in which experiences a reversible transition to cubic γ-Li_2TiO_3 [8, 14-17]. A higher order structural phase transition of monoclinic phase at about 450 ˚C was also reported by Hoshino et al. using X-ray diffraction method at high temperatures [18]. The cationic arrangement of ($LiTi_2$) layers in Li_2TiO_3 ceramic was precisely revealed through structure refinement of single-crystal X-ray diffraction method by Kataoka et al. [19]. The synthesized Li_2TiO_3 powders are usually characterized by a large grain size and inferior sintering characteristics [8]. In addition, porous microstructure due to sublimation of lithium [9, 20] and crack formation due to phase transition under high sintering temperatures (above 1150˚C) [9, 21] adversely affect the densification of Li_2TiO_3. Therefore, reducing the sintering temperature is very important to control the above-mentioned defects. Several approaches have been applied to enhance the sintering characteristics of ceramics like doping [22-24], addition of sintering aids with

[DOI: 10.22068/ijmse.16.1.1]

low melting points [25-28], using wet chemistry synthesis methods (hydrothermal, sol-gel,…) [29, 30], and making beneficiary from non-stoichiometry effects [8, 21]. Improvement in sintering behavior in nonstoichiometric $Li_{2+x}TiO_3$ [8] is attributed to the creation of vacancies in solid state sintering and defect chemistry which is responsible for accommodating excess Li_2O, somehow, as for $x < 0.08$, Li_i^+ defects are created, and for $x > 0.1$, Li_{Li}^+ are formed along with simultaneous formation of V_{Ti}^{4-} and V_O^{2+} defects, providing charge compensation. The effects of the hydrogen atmosphere on non-stoichiometry of Li_2TiO_3 and addition of some oxide additives to control oxygen defects was examined by Hoshino et al. [31]. Murphy et al. [16] used density functional theory to calculate formation energies for the intrinsic defect species and therefore identify the mechanisms responsible for accommodating both excess Li_2O and TiO_2 across a wide range of temperatures and oxygen partial pressures. Huang et al. [11] studied the effects of ZnO addition with 10-50 mol.% and reported new microwave dielectric material of $0.7Li_2TiO_3$–$0.3ZnO$ with good combination of dielectric properties of εr of ~22.95, Q×f of ~99,800 GHz (measured at 8.91 GHz), and a τf of ~0 ppm/◦C.

The aim of the present work was to study the effects of ZnO addition with lower values of 0.5-5 mol.% and to explore whether Zn^{2+} ions (as well as Li^+ ions) can be accommodated in Li_2TiO_3 lattice and therefore be responsible for alteration of mass transfer and diffusion rate during sintering process through formation of ionic defects. Furthermore, the effects of ZnO addition on the structure, microstructure and microwave dielectric properties of Li_2TiO_3 ceramics were investigated.

2. EXPERIMENTAL PROCEDURE

Li_2CO_3 (Sigma Aldrich, 13010, 99% purity) and TiO_2 (Merck, 1.00808.1000, >99% purity) were ground in a PM 400 Retsch planetary ball mill using tungsten carbide vials and balls at 300 rpm in order to synthesize stoichiometric Li_2TiO_3 powder. The ball-to-powder ratio of 10:1 and milling duration of 5 h were employed. The milled powders were subject to calcination in an electrical box furnace at temperature of 700˚C with 4 h holding time at maximum temperature and heating rate of 5 ˚C/min. ZnO powder (Sigma Aldrich, 205532, 99.9% purity) was added to Li_2TiO_3 powder in order to prepare Li_2TiO_3 + xZnO samples that x values were adopted as 0, 0.5, 1, 1.5, 2, 3, and 5 mol%. All starting materials were dried prior to weighing at 200 ˚C for 2 h in order to remove moisture. The slurries were dried at 90 ˚C for 4 h and then at 180 ˚C for 4 h. Different batches were granulated with PVA as binder and then were pressed into pellets under pressure of 200 MPa. Sintering process was performed in an electrical box furnace at temperatures between 1050-1250˚C with heating rate of 10 ˚C/min and holding temperature of 3 h at maximum temperature under ambient atmosphere. Green parts were muffled with powder of the same composition in order to avoid Li sublimation during sintering. The bulk Density and porosity of pellets were measured by Archimedes method (ASTM-C373-88). The phase identification was performed through X-Ray Diffraction (XRD) patterns obtained by Philips PW 3710 with Cu-kαline (40 kV, 30 mA). The data were collected in the 2θ range of 5-80˚. The microstructural analysis of samples were performed by means of field emission scanning electron microscope (FE-SEM) (TESCAN MIRA 3 LMU). The samples were polished and then thermally etched at 50 ˚C lower than sintering temperature for 30 min. Raman spectra have been recorded by DXR-Smart Raman (Thermo-scientific) instrument with Smart Excitation Laser (Thermo Scientific) with laser wavelength at 780 nm. Resolution, number of scans and integration time were 2 cm^{-1}, 5 and 1500 s, respectively. Microwave dielectric properties were measured in the frequency range of 8–10 GHz and diameter-to-thickness ratio of the DR was adjusted to ≈ 2.26 for assurance of the first resonance mode to be of the TE01δ-type. The DR was placed on the low-loss quartz support of 5 mm diameter and 4.3 mm height in the center of the silver-clad cylindrical resonance cavity (QWED, Poland) having inner diameter of 24 mm and height of 16 mm. The microwave resonances in transmission mode (s^{21} parameter) were measured using HP8719C vector network analyzer. The dielectric constant (εr) was calculated using the QWED software 37 which takes into account the geometry of the DR and the metal enclosure. The unloaded Q-factor was calculated according to Eq. 1 [32]:

[DOI: 10.22068/ijmse.16.1.1]

$$Q = \frac{Q_L}{1 - 10^{-P/20}} \qquad (1)$$

where Q_L is the loaded quality factor determined from the full width of the resonance peak at the 3 dB level, and P is the absolute value of the s^{21} parameter at the resonance in dB. To minimize the coupling, the s^{21} parameter at the resonance peak was adjusted to around −30 dB. Because no corrections for conduction loss were included in the calculations, the Q × f reported represent the lower bound value. The temperature coefficient of resonant frequency τf was also measured in the temperature range from 25 ˚C to 75 ˚C.

3. RESULTS AND DISCUSSION

Fig. 1a demonstrates the density evolution of Li_2TiO_3 + xZnO ceramics sintered at 1100˚C which shows a slight decrease after addition of 0.5 mol% ZnO and then density improvement for x up to 2 mol% with a change towards lower densities for higher values of x ≥ 3. The maximum density of 99% (3.33 g/cm^3) 98.94% (3.33 g/cm^3) is related to Li_2TiO_3 + 2ZnO sample sintered at low sintering temperature of 1100˚C. Temperature variations of density of Li_2TiO_3 + xZnO samples (x = 0, 2, 3) are presented in Fig. 1b which reveal that density reaches the maximum value at 1100˚C and remains almost unchanged for all specimens until 1200˚C and further increase in temperature to 1250˚C decreases the density of ceramics.

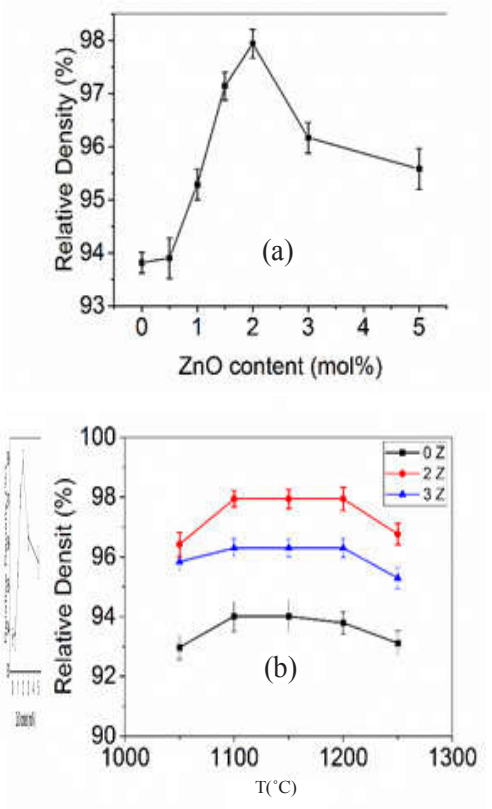

Fig. 1. Density Relative density of (a) Li_2TiO_3 + xZnO (x = 0-5) ceramics sintered at 1100˚C and (b) Li_2TiO_3 + xZnO (x = 0, 2, 3) at different temperatures for 3 h

The addition of ZnO into Li_2TiO_3 in the present investigation is considered as doping which has resulted in the enhancement of sintering behavior of ceramic through formation of point defects in solid state sintering Fig. 2.

Fig. 2. Schematic representation of vacancy diffusion mechanism after addition of ZnO

[DOI: 10.22068/ijmse.16.1.1]

Fig. 3 represents room temperature XRD patterns recorded from Li_2TiO_3 + xZnO ceramics sintered at 1100 ˚C. All present peaks are assigned to monoclinic β-Li_2TiO_3 phase (JCPDS card: 330831) with rock salt structure. The formation of solid solution between Li_2TiO_3 and ZnO has been reported by Huang et al. [16] in which higher values of ZnO content in (1-x)Li_2TiO_3–xZnO ceramic system (x = 0.1-0.5) were investigated in order to alter the τf value of ceramic to zero.

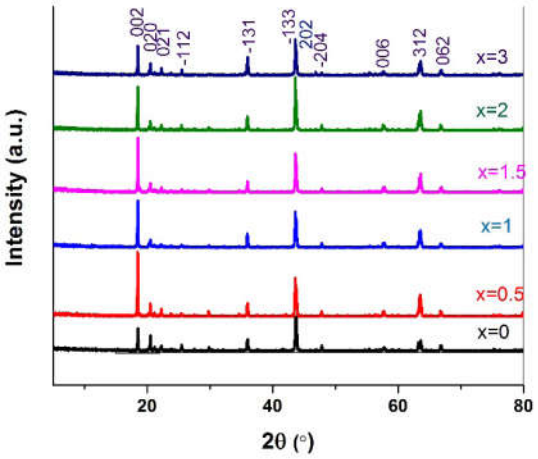

Fig. 3. The XRD patterns of sintered Li_2TiO_3 + xZnO samples.

In order to examine the structural changes of the ceramic after ZnO addition, Rietveld refinement has been performed by the MAUD Software [33, 34]. Before refinement the program has been calibrated to consider the instrumental zero shift and asymmetry of instrument using XRD pattern of Si standard sample (NBS 640) free from the effect of small crystallite size broadening and lattice defects (micro-strain) [35]. The most reliable part of XRD patterns (2θ=25-60) has been determined and utilized for refinement. The CIF file of Li_2TiO_3 with monoclinic crystal structure has been applied for refinement. The GOF values ($\chi=\sqrt{R_{wp}^2/R_{exp}^2}$) less than 2 are representative of a good fitting and Table 1 confirms the reliability of refinement. To more support the reliability of refinement results, the differences of the experimental and calculated pattern are also illustrated in Fig. 4a for some samples. It could be seen that the differences are almost zero in whole 2θ which is indication of good refinement.

The results clearly indicate that the cell volume reduced with Zn addition (Table 1, Fig. 4b). This result may be related to the creation of vacancies in the structure and therefore increases diffusion rate in the lattice.

Table 1. Cell volume and lattice parameters of different Li_2TiO_3 + xZnO samples obtained by Rietveld refinement method as well as GOF factor of refinement.

ZnO	a (Å)	B (Å)	C (Å)	β °	V (Å^3)	χ
0	5.069	8.798	9.765	100.19	428.56	1.009
0.5	5.067	8.795	9.763	100.22	428.23	1.107
1	5.068	8.793	9.765	100.21	428.29	1.031
1.5	5.068	8.794	9.763	100.21	428.23	1.075
2	5.067	8.793	9.765	100.21	428.21	1.198
3	5.068	8.794	9.761	100.22	428.16	1.078

[DOI: 10.22068/ijmse.16.1.1]

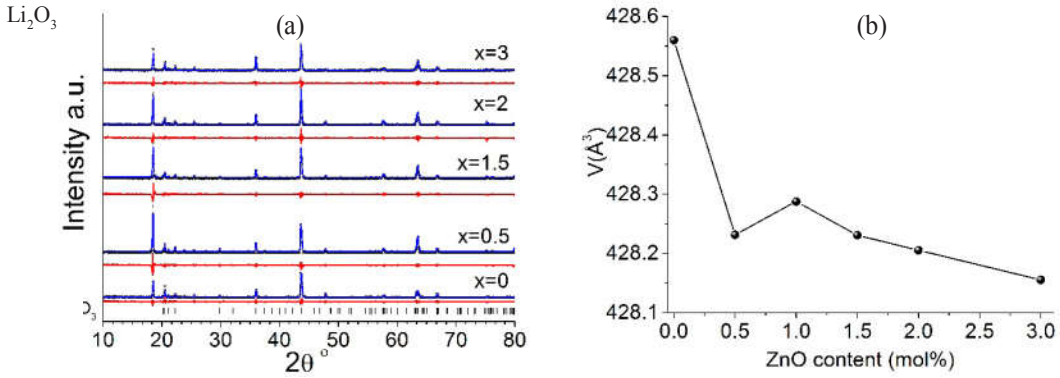

Fig. 4. (a) The differences of the experimental and calculated pattern and (b) The cell volume of Li_2TiO_3 + xZnO obtained by Rietveld refinement.

Simulated XRD patterns by MAUD software (Fig. 5) also showed that the intensity of 002 diffraction line (2θ~18.5o) is decreased by Zn incorporation while intensity of 202 and 33 diffraction lines (2θ~ 43.6 o) are enhanced. Literature related the changes of the intensity to the solely change in ordering [11]; however, one should consider that addition of Zn also modifies the structure factor and scattering intensity.

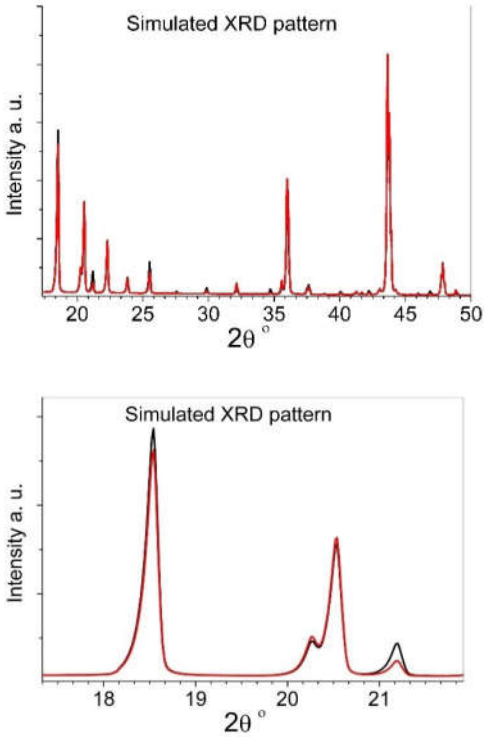

Fig. 5. Simulated XRD patterns of Li_2TiO_3 +5ZnO

Raman spectra of the prepared samples (Fig. 6) verify the phase purity. Since these spectra are very similar no more information could be obtained by them. In Li_2TiO_3, the frequencies within 700–550 cm-1, 400–550 cm^{-1}, and 250–400 cm^{-1} region are assigned to Ti-O stretching in TiO6 octahedral, Li-O stretching in tetrahedral, and Li-O stretching in octahedral coordinations, respectively. In the Li_2TiO_3 structure, the lithium can occupy both octahedral and tetrahedral positions [36].

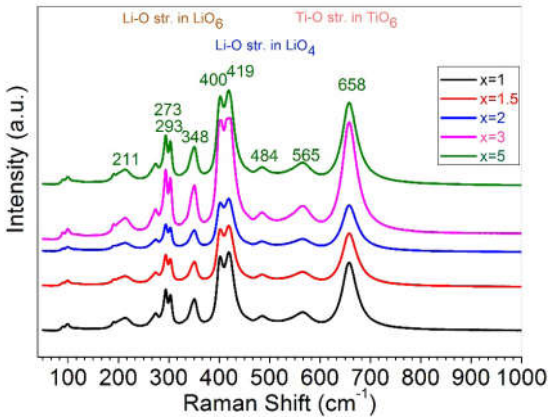

Fig. 6. Raman spectra of Li_2TiO_3 + xZnO ceramics measured at ambient temperature

The SEM micrographs of thermal-etched Li_2TiO_3 + xZnO samples sintered at 1100 ˚C are illustrated in Fig. 7. The surface morphology of pure Li_2TiO_3 (Fig. 7a) reveals the occurrence of abnormal grain growth. Microstructural refinement is evident

[DOI: 10.22068/ijmse.16.1.1]

for ceramics with x < 1.5 from the SEM images in Fig. 7a-c. Free energy of the system associated with grain boundaries provides the driving force for grain growth. Solute ions in crystalline systems impose a retarding force for migration as the boundary migration results in an asymmetric dopant concentration profile due to different diffusivity of the solute ions from that of the host across the boundary [37]. The ceramic with x = 2 possesses a good close packing of grains (Fig. 7e) and highest value of density ρ = 3.33 g/cm^3 with grain size within a narrow range. Further increase in dopant concentration in Li_2TiO_3 + 3ZnO caused an upturn in grain size of the ceramic with preferential grain growth. It is also visible that the porosities have grown along with grain growth. Li_2TiO_3 + 5ZnO microstructure demonstrates the continual trend of increase in grain size and pore size as well. The presence of porosities due to the lithium sublimation is also observed in micrographs.

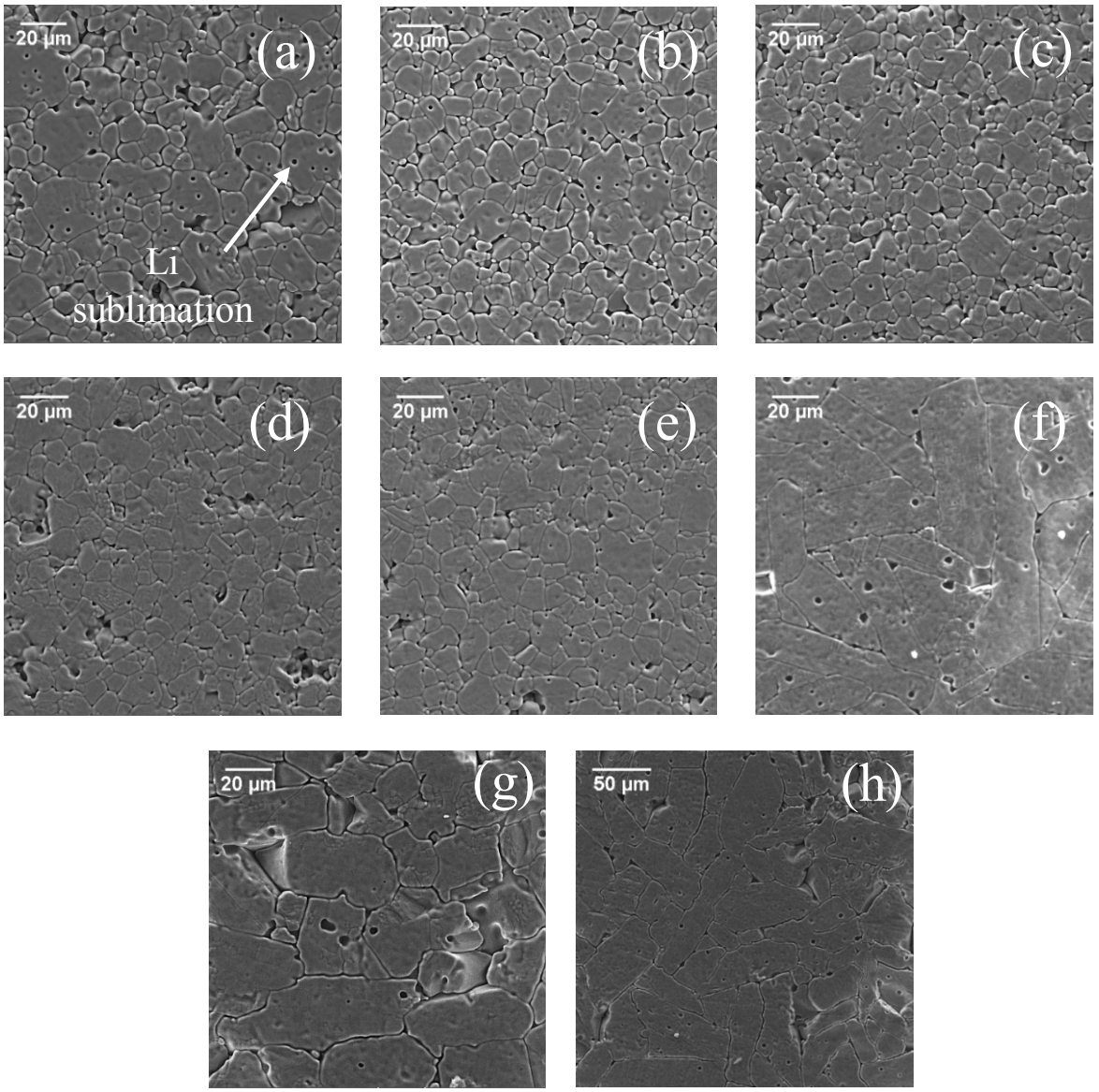

Fig. 7. SEM micrographs of Li_2TiO_3 + xZnO pellets sintered at 1100 ˚C for different values of x (a) 0, (b) 0.5, (c) 1, (d) 1.5, (e) 2, (f) 3 (g) and (h) 5 (two different magnifications).

[DOI: 10.22068/ijmse.16.1.1]

Fig. 8 contains the microstructures of Li_2TiO_3 + 3ZnO ceramic sintered at 1000 ˚C that shows the existence of spot like areas containing Zn distributed uniformly through the microstructure.

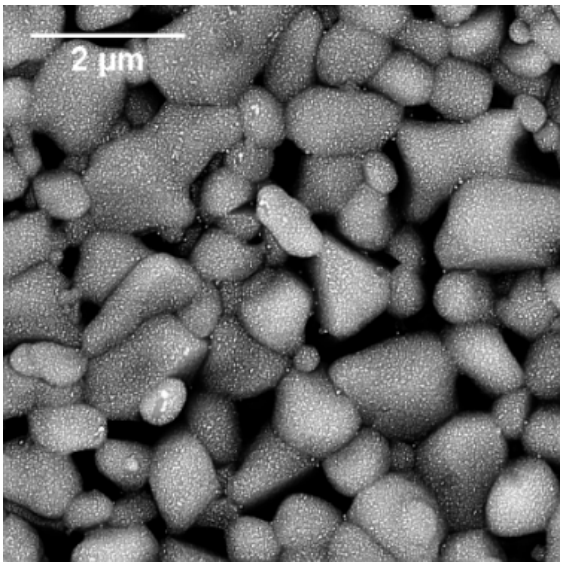

Fig. 8. SEM micrographs (back scattered mode) of Li_2TiO_3 + 3ZnO pellets sintered at 1000˚C

Fig. 9a plots the dielectric constant of the Li_2TiO_3 + xZnO ceramics as a function of ZnO addition. The relationships between dielectric constant and ZnO content reveal the same trend as those observed between density and ZnO content, since it increases as the ZnO content increases up to the value of 2 mol%. Li_2TiO_3 + 2ZnO ceramic with the maximum density represents the highest value of εr = 22.5 and then dielectric constant decreased with further increase in ZnO content due to higher porosities in the ceramic (Fig. 7f and g). Therefore, it can be concluded that the dielectric constant of the system under study is mainly controlled by density in agreement with Clausius–Mossotti equation. This equation related the dielectric constant of ceramic to the dipoles in unit cell volume and dielectric polarizabilities of ions [9]. In another word, the higher the density of ceramic, the higher the dipoles in a unit cell volume and therefore the higher the value of εr [9, 20]. The relation can be expressed in another way as the εr increases with higher density and lower porosities because of the unity of εr of air [8].

Fig. 9b presents the quality factor (Q × f) of the Li_2TiO_3 + xZnO ceramics as a function of ZnO concentration. The quality factor of the ceramic has deteriorated through lower values of ZnO doped into the structure in compositions of Li_2TiO_3 + xZnO (x = 0.5, 1, and 1.5 mol%). The reason may be related to the finer microstructure of ceramics presented in Fig. 7b-d. Slight improvement in Q × f values was observed with increase in ZnO content up to 1.5 mol%, while Li_2TiO_3 + 2ZnO ceramics showed uprising in quality factor due to density improvements and uniform microstructure. However, the increase in Q × f value continued for Li_2TiO_3 + 3ZnO which can be explained by excessive grain growth of the ceramic. The maximum value of Q × f = 31800 GHz was obtained for Li_2TiO_3 + 3ZnO sample. The decrease in Q × f value of Li_2TiO_3 + 5ZnO may be related to the formation of large pores as well as large grains in the microstructure.

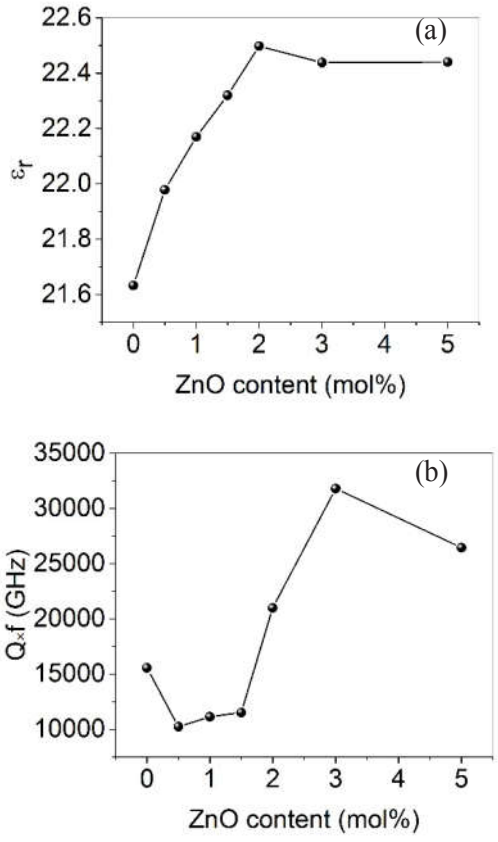

Fig. 9. Variation of (a) dielectric constant and (b) quality factor of Li_2TiO_3 + xZnO ceramics sintered at 1200 ˚C vs. ZnO amounts

[DOI: 10.22068/ijmse.16.1.1]

Fig. 10 illustrates the variation of Q × f of Li_2TiO_3 + 3ZnO ceramic with respect to sintering temperature. Quality factor increased during sintering up to 1100˚C with slight difference until 1200˚C and then decreased at sintering temperature of 1250 ˚C as a result of decrease in density

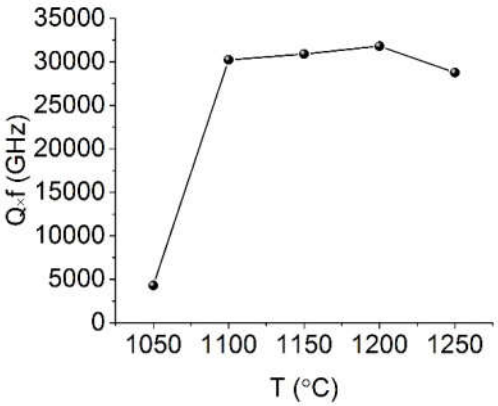

Fig. 10. Variation of quality factor of Li_2TiO_3 + 3ZnO, vs. sintering temperature

The temperature coefficient of resonant frequency, τf of pure Li_2TiO_3 sintered at 1200˚C was measured +26 ppm/˚C which decreased to +13 ppm/˚C in Li_2TiO_3 + 3ZnO ceramic. The temperature coefficient of resonant frequency is mainly controlled by the composition, the additives, and the second phase of the materials [11]. The reduction in τf value of Li_2TiO_3 was also reported in [11] with higher values of ZnO addition (10-50 mol.%) .

4. CONCLUSIONS

The influence of ZnO addition on the densification, crystal structure, microstructure and microwave dielectric properties of Li_2TiO_3 + xZnO (x = 0-5) was explored in this experiment. It was found that density increases with increasing the ZnO content (x ≤ 2), since material transport is facilitated through lattice defects formed through Zn substitution in the ceramic structure. The substitution of Zn into host lattice caused decrease in cell volume proved by Rietveld refinement method which verifies that Zn tends to replace Li cationic site than incorporate in tetrahedral interstitial sites or Ti cationic site. Simulated XRD patterns also showed that the intensity of 002 diffraction line (2θ~18.5o) is decreased by Zn incorporation (replacement of Li cationic sites) while intensity of 202 and 33 diffraction lines (2θ~ 43.6 o) are enhanced. The maximum density of 3.33 g/cm3 was obtained after sintering of Li_2TiO_3 + 2ZnO ceramic at low temperature of 1100 ˚C. Further increase in dopant concentration (x ≥ 3) resulted in lower densities due to development of porosity in the microstructures. These two ceramics (Li_2TiO_3 + 3ZnO and Li_2TiO_3 + 5ZnO) developed completely different microstructures containing large grains. The best dielectric constant of 22.5 was achieved for Li_2TiO_3 + 2ZnO ceramic, and the highest Q × f of ~ 31800 GHz was measured for Li_2TiO_3 + 3ZnO ceramic which had a microstructure containing the large grains.

5. ACKNOWLEDGEMENT

This work was sponsored by Ministry of Science, Research and Technology of Iran under the PhD project, with grant no. 381392058, at Materials & Energy Research Center (MERC).

REFERENCES

1. Zhang, Y., Y. Zhang, and M. Xiang, "Crystal structure and microwave dielectric characteristics of Zr-substituted $CoTiNb_2O_8$ ceramics". Journal of the European Ceramic Society, 2016, 36, 1945-1951.
2. Lin, Y. J., Wang, S. F., Lai, B. C., Liu., Y. X, Chang, Y. L. and Yang, J. R., "Densification, microstructure evolution, and microwave dielectric properties of $Mg_{1-x}Ca_xZrTa_2O_8$ ceramics." Journal of the European Ceramic Society, 2017, 37, 2825-2831.
3. Ullah, A., Liu, H., Hao, H., Iqbal, J., Yao , Z. and Cao, M, "Influence of TiO_2 additive on sintering temperature and microwave dielectric properties of $Mg_{0.90}Ni_{0.1}SiO_3$ ceramics." Journal of the European Ceramic Society, 2017, 37, 3045-3049.
4. Takahashi, S., Kan, A. and Ogawa, H., "Microwave dielectric properties and crystal structures of spinel-structured $MgAl_2O_4$ ceramics synthesized by a molten-salt method." Journal of the European Ceramic Society, 2017, 37, 1001-1006.

[DOI: 10.22068/ijmse.16.1.1]

5. Xiang, H., Li, C., Tang, Y. and Fang, L., "Two novel ultralow temperature firing microwave dielectric ceramics $LiMVO_6$ (M = Mo, W) and their chemical compatibility with metal electrodes." Journal of the European Ceramic Society, 2017, 37,3959-3963.
6. Yuan, L. L. and J. J. Bian, "Microwave Dielectric Properties of the Lithium Containing Compounds with Rock Salt Structure." Ferroelectrics, 2009, 387, 123-129.
7. Bian, J. J. and Dong, Y. F., "New high Q microwave dielectric ceramics with rock salt structures: (1−x) Li_2TiO_3+xMgO system (0≤x≤0.5)." Journal of the European Ceramic Society, 2010, 30, 325-330.
8. Hao, Y. Z., Zhang, Q. L, Zhang, J., Xin. C. R. and Yang. H., "Enhanced sintering characteristics and microwave dielectric properties of Li_2TiO_3 due to nano-size and nonstoichiometry effect." Journal of Materials Chemistry, 2012,22, 23885-23892.
9. Hao, Y. Z., Yang, H., Chen, G. H. and Zhang, Q. L., "Microwave dielectric properties of Li_2TiO_3 ceramics doped with LiF for LTCC applications." Journal of Alloys and Compounds, 2013, 552, 173-179.
10. Fu, Z. F., P. Liu, and J. L. Ma, "Fabrication nanopowders by high-energy ball-milling and low temperature sintering Li_2TiO_3 microwave dielectrics." Materials Science and Engineering: B, 2015. 193, 32-36.
11. Huang, C. L., Y. W. Tseng, and J. Y. Chen, "High-Q dielectrics using ZnO-modified Li_2TiO_3 ceramics for microwave applications." Journal of the European Ceramic Society, 2012, 32, 3287-3295.
12. Chen, G. h., Hou, M. Z. and Yang, Y. "Microwave dielectric properties of low-fired Li_2TiO_3 ceramics doped with Li_2O–MgO–B_2O_3 frit." Materials Letters, 2012, 89, 16-18.
13. Bian, J. J., Wang, L., and Yuan, L. L., "Microwave dielectric properties of $Li_{2+x}Ti_{1-4x}Nb_{3x}O_3$ (0≤x≤0.1)." Materials Science and Engineering: B, 2009, 164,96-100.
14. Fehr, T. and E. Schmidbauer, "Electrical conductivity of Li_2TiO_3 ceramics." Solid State Ionics, 2007, 178, 35-41.
15. Laumann, A., Jensen, K. M. O., Tyrsted, C., Bremholm, M., Fehr, K. T., Holzapfel, M. and Iversen, B. B., "In-situ Synchrotron X-ray Diffraction Study of the Formation of Cubic Li_2TiO_3 Under Hydrothermal Conditions," European Journal of Inorganic Chemistry, 2011,14, 2221-2226.
16. Murphy, S. T. and N. D. Hine, "Point Defects and Non-stoichiometry in Li_2TiO_3." Chemistry of Materials, 2014, 26, 1629-1638.
17. Laumann, A., Fehr, K. T., Boysen, H. Hoelze, M. and Holzapfel, M., "Temperature-dependent structural transformations of hydrothermally synthesized cubic Li_2TiO_3 studied by in-situ neutron diffraction." Zeitschrift für Kristallographie Crystalline Materials, 2011, 226, 53-61.
18. Hoshino, T., Tanaka, K., Makita, J. and Hashimoto, T., "Investigation of phase transition in Li_2TiO_3 by high temperature X-ray diffraction." Journal of Nuclear Materials, 2007, 367, 1052-1056.
19. Kataoka, K., Takahashi, Y., Kijima, N., Nagai, H., Akimoto, J., Idemoto, Y. and Ohshima, K. I., "Crystal growth and structure refinement of monoclinic Li_2TiO_3." Materials Research Bulletin, 2009, 44, 168-172.
20. Liang, J., Lu, W., Lei, W., Fan, G. and Ma, H., "A new route to improve microwave dielectric properties of low-temperature sintered Li_2TiO_3-based ceramics." Journal of Materials Science: Materials in Electronics, 2013,24, 3625-3628.
21. Bian, J. J. and Dong, Y. F., "Sintering behavior, microstructure and microwave dielectric properties of $Li_{2+x}TiO_3$ (0≤x≤0.2)." Materials Science and Engineering: B, 2011, 176, 147-151.
22. Wang, J., Yue, Z., Gui, Z. and Li, L., "Low-temperature sintered $Zn(Nb_{1-x}V_{x/2})_2O_{6-2.5x}$ microwave dielectric ceramics with high Q value for LTCC application." Journal of alloys and compounds, 2005, 392, 263-267.
23. Zhang, J., Y. Zhou, and Z. Yue, "Low-temperature sintering and microwave dielectric properties of LiF-doped $CaMg_{1-x}Zn_xSi_2O_6$ ceramics." Ceramics International, 2013,39, 2051-2058.
24. Pei, J., Yue, Z., Zhao, F., Gui, Z. and Li, L., "Microwave dielectric ceramics of hexagonal $(Ba_{1-x}A_x)La_4Ti_4O_{15}$ (A= Sr, Ca) for base station applications." Journal of Alloys and Compounds, 2008, 459, 390-394.
25. Bai, X. J., Liu, P., Fu, Z. F, Guo, B. C, "Low-temperature sintering and microwave dielectric properties of LiF-doped $Ba(Mg_{1/2}W_{1/2})O_3$–TiO_2 ceramics." Journal of Alloys and Compounds, 2016, 667, 146-150.
26. Sayyadi-Shahraki, A., Taheri-Nassaj, E., Hassanzadeh-Tabrizi, S. A. and Barzegar-Bafrooei, H., "Microwave dielectric properties and chemical compatibility with silver electrode of Li_2TiO_3 ceramic with Li_2O–ZnO–B_2O_3 glass additive." Physica B: Condensed Matter, 2015,457, 57-61.
27. Liang, J. and W.-Z. Lu, Microwave Dielectric Properties of Li_2TiO_3 Ceramics Doped with

[DOI: 10.22068/ijmse.16.1.1]

$ZnO-B_2O_3$ Frit. Journal of the American Ceramic Society, 2009, 92, 952-954,

28. Liang, J., Lu, W. Z., Wu, J. M. and Guan, G. J., "Microwave dielectric properties of Li_2TiO_3 ceramics sintered at low temperatures." Materials Science and Engineering: B, 2011, 176, 99-102.
29. Hu, C. and P. Liu, "Preparation and microwave dielectric properties of SiO_2 ceramics by aqueous sol–gel technique." Journal of Alloys and Compounds, 2013, 559, 129-133.
30. Wang, H., Zhang, Q., Yang, H. and Sun, H., "Synthesis and microwave dielectric properties of $CaSiO_3$ nanopowder by the sol–gel process." Ceramics International, 2008, 34, 1405-1408.
31. Hoshino, T., Tsuchiya, K., Hayashi, K., Terai, T., Tanaka, S. and Takahashi, Y., "Non-stoichiometry of Li_2TiO_3 under hydrogen atmosphere conditions." Fusion Engineering and Design, 2005, 75–79, 939–943.
32. Kolodiazhnyi, T., "Origin of extrinsic dielectric loss in 1:2 ordered, single-phase $BaMg_{1/3}Ta_{2/3}O_3$." Journal of the European Ceramic Society, 2014, 34, 1741-1753.
33. Gialanella, S. and L. Lutterotti, "On the measure of order in alloys." Progress in Materials Science, 1997, 42, 125-133.
34. Lutterotti, L., Ceccato, R., Maschio, R., Pagani, E., "Quantitative analysis of silicate glass in ceramic materials by the Rietveld method. in Materials Science Forum." 1998, Aedermannsdorf, Switzerland: Trans Tech Publications, 87-92
35. Torkaman, N. M., Ganjkhanlou, Y., Kazemzad, M., Dabaghi, H. H., Keyanpour-Rad, M., "Crystallographic parameters and electro-optical constants in ITO thin films." Materials Characterization, 2010. 61, 362-370.
36. Nakazawa, T., Naito, A., Aruga, T., Grismanovs, V., Chimi, Y., Iwase, A. and Jitsukawa, S., "High energy heavy ion induced structural disorder in Li_2TiO_3." Journal of Nuclear Materials, 2007,367–370, 1398-1403.
37. Yoshida, H., Nagayama, H. and Sakuma, T., "Small dopant effect on static grain growth and flow stress in superplastic TZP", Materials Transactions, 2003, 44,935-939.

[DOI: 10.22068/ijmse.16.1.1]